



Journal of Applied Sciences

ISSN 1812-5654

science
alert

ANSI*net*
an open access publisher
<http://ansinet.com>

Assessment of a Technique for the Torsional Response Reduction of Seismic Isolated Asymmetric Structures

¹M. Adibramezani, ²A.S. Moghadam and ²M. Ziyaeifar

¹Science and Research Branch, Islamic Azad University, Tehran, Iran

²International Institute of Earthquake Engineering and Seismology,
No. 26, North Dibji, Dr. Lavasani Street Tehran, Iran

Abstract: This research studies the effectiveness of a bilinear hysteric elastomeric base-isolation system in decreasing the torsional moments generated in a superstructure due to the bidirectional actions of selected ground motions. A five-storey three-dimensional steel structure with asymmetry in both horizontal directions is assumed as the basic model. A parametric study shows that assuming an L-shaped plan for the buildings leads to more critical results. The eccentricity of the L-plan building is changed to a wide range of plan dimensions. Seven ground motions are selected based on the site specifications and the distance of the site to the fault rupture. The mean peak responses are compared to the corresponding responses of the fixed base system to investigate the effectiveness of base isolation. They are also compared with those of the corresponding symmetric system to highlight the effect of torsional coupling. The effects of the center of stiffness of the isolation system being coincident with the superstructure's center of mass are investigated as a technique for reducing the response. The torsional moments are shown to be reduced even in cases with large structural eccentricities and the response reduction has a greater impact in the lower storeys. When the superstructure's center of mass coincides with the base-isolation system's center of stiffness, this causes a reduction in the relative displacement of the exterior edges, the storey rotation and the amount of damage. Therefore, eliminating asymmetry at the base level is proposed as a practical tool to enhance the performance of asymmetric base-isolated buildings.

Key words: Torsional responses, base isolation, eccentricity, rubber bearing, elastomeric bearing

INTRODUCTION

The application of isolation techniques may reduce or eliminate damage to buildings and their contents during an earthquake. This technique is now recognized as a mature and efficient technology and can be adopted to improve the seismic performance of important buildings such as schools, hospitals and industrial structures, in addition to structures where sensitive equipment needs to be protected during an earthquake. The seismic vulnerability of asymmetric structures as a result of the dynamic amplification of the torsional component of the seismic response has been repeatedly demonstrated for strong earthquakes. In general, an isolator system is equipped with two key features: flexibility and energy absorbing capacity. Flexibility elongates the period of the structure, thereby reducing the earthquake forces on the system, while the energy absorbing capacity reduces both the seismic energy and the relative displacements that are transmitted to the structure. The isolator system increases

the fundamental period of the structure, shifting it out of the region of the dominant earthquake energy, while at same time increasing the damping capacity of the structure. The structure's response can be efficiently adjusted by tuning the isolation system's characteristics. Horizontally flexible support and the ability to dissipate a considerable amount of energy are essential features of the base-isolation system. Buildings with an asymmetric distribution of stiffness and strength are especially vulnerable during earthquakes, as was demonstrated by the partial or total collapse of many such structures during the Mexico earthquake (Chandler, 1986). Several investigations have addressed the torsional coupling in structures with elastomeric isolation systems. However, their conclusions have been generally restricted to the particular systems analyzed, which is evident from the following review of earlier studies.

It is concluded that dynamic torque amplification, which is the ratio of dynamic torque to static torque at the Center of Stiffness (CS) of the superstructure, is small or

negligible (Lee, 1980). It was also shown that the additional corner displacements due to torsion were small and were within 30% of the lateral displacement at the corner of the base, provided the eccentricity of the isolation system is also small ($\leq 0.2 L$; L : Longest plan dimension) even for large superstructure eccentricities ($\leq 0.4 L$). These conclusions were based on the study of single-storey structures having four corner columns and elastomeric isolators with masses concentrated at each corner. The model used had an excessively large radius of gyration of mass ($\leq 0.7 L$) and the isolators consisted of two laterally independent bilinear hysteretic springs. Thus, the nonlinear biaxial interaction between the two directions was neglected (Lee, 1980).

Pan and Kelly used a rigid superstructure model with linear isolators that had an equivalent damping of 8-10%. They concluded that the effect of torsional coupling on the seismic response of base-isolated structures with small eccentricities is insignificant, as a result of the combined effects of the time lag between the maximum lateral and torsional response and the influence of the high damping in the isolation system (Pan and Kelly, 1983).

Eisenberger and Rutenberg also concluded that when the eccentricity in the isolation system approaches zero, the torsional response is virtually eliminated, even for large superstructure eccentricities ($0.16L$). These conclusions were determined by re-examining the validity of the findings in the aforementioned studies using an equivalent 3D analysis of multi-storey structures with bilinear isolators without biaxial interaction (Eisenberger and Rutenberg, 1986).

From an experimental study of a single-storey torsionally stiff base-isolated structure (ratio of uncoupled torsional to lateral frequency = 1.7) with an elastomeric isolation system, Nakamura concluded that for moderate superstructure and isolation system eccentricities ($0.1 L$), the amplification of torsional motions is small or negligible in elastomeric base-isolated structures. However, this conclusion is restricted to torsionally stiff base-isolated structures (Nakamura *et al.*, 1989).

Nagarajaiha *et al.* (1993) studied torsion in multi-storey base-isolated structures with inelastic elastomeric isolation systems subject to bidirectional lateral ground motions of the 1940 El-Centro and 1952 Taft earthquakes. It is concluded that the superstructure eccentricity has a significant influence on the torsional amplification and also concluded that the dynamic torque amplification could be as high as 4.0 for superstructure eccentricities of $\sim 0.1 L$.

Jangid and Datta (1994) studied the nonlinear response of torsionally coupled base-isolated systems subjected to random ground excitation. The base isolator consisted of an array of elastomeric bearings assumed to have elasto-plastic hysteretic behaviour. They concluded that the effectiveness of the torsionally coupled base isolation system is less than that of the corresponding symmetric system, especially in reducing the superstructure's displacement perpendicular to the direction of eccentricity. They found that for higher eccentricities of the superstructure, the effectiveness of the base isolation system is reduced. However, the eccentricity of the superstructure did not have a significant influence on the base displacement. They also found that increasing the yield strength of the isolator decreased the effectiveness of the base isolation system (Jangid and Datta, 1994).

Almazan and De la Llera (2000) studied the torsional response of symmetric but slender structures isolated with the Friction Pendulum System (FPS) and found that when the slenderness ratio of the structure increased, the torsional stiffness decreased and the non-uniform distribution of lateral displacements increased.

Tena-Colunga and Gómez-Soberón (2002) studied a structure with eccentricities in both the superstructure and the lead-rubber bearing isolation system. They concluded that for all corner isolators, the ratios of the peak displacements of the isolators when subjected to bidirectional seismic and unidirectional input due to static eccentricities strongly depend on directivity and other characteristics of each ground motion component. Furthermore, the relative ratio between the peak isolator displacements for bidirectional eccentricities and the unidirectional eccentricities is more complex and is dependent on many parameters. Among these are: (1) dynamic coupling of the base-isolated structure with the ground motion, (2) eccentricity ratio for the isolation system, (3) torsional response of the isolation system, which is greatly affected by the torsional response of the superstructure and (4) the location of a given isolator (Tena-Colunga and Gómez-Soberón, 2002).

Samali *et al.* (2003) studied the dynamic characteristics and responses of a five storey benchmark model with moderate mass eccentricities using a shaking table, simulating four different ground motions. Laminated rubber bearings and lead core rubber bearings were compared to the translational and torsional responses of the benchmark model. Both the translational and torsional responses were significantly reduced with the addition of either Laminated Rubber Bearing (LRB) or Lead Core Rubber Bearing (LCRB) isolated systems, regardless of the nature of the ground motion input. The LRBs were

found to be more effective than the LCRBs in reducing model relative displacements, the relative torsional angle and the accelerations and therefore, provided better protection to the superstructure and its contents. The coupling effects of lateral and torsional responses were evaluated for a five storey steel frame with an eccentricity of 0.125 L. The LRBs were found to be similar to the LCRBs in preventing torsional deformation of the model, but were more effective than the LCRBs in reducing the relative displacements and accelerations (Samali *et al.*, 2003).

Ryan and Chopra (2004) presented a procedure based on non-linear analysis that estimates the peak deformation among all isolators in an asymmetric building subjected to strong ground motion. The governing equations were reduced to a form such that the median normalized deformation from a number of ground motions with a given period depends primarily on four global parameters of the isolation system: the isolation period, the normalized strength, the torsional-to-lateral frequency ratio and the normalized stiffness eccentricity. The design equation conservatively estimated the peak deformation among all isolators, but was generally within 10% of the exact value. Its performance was superior to the non-linear uniform building code procedure, which significantly underestimated the peak isolator deformation (Ryan and Chopra, 2004).

Llera *et al.* (2005) studied the torsional balance of elastic asymmetric structures with frictional dampers. The torsional balance concept is defined as minimising the correlation between the translation and rotation of the building plan. An explicit equation to achieve this condition in the case of linear, nonlinear, single, or multi-storey structures was presented. Lateral-torsional coupling is controlled with frictional dampers by placing the so-called Empirical Center of Balance (ECB) of the structure at equal distances from all edges of the building. This approach was developed for single storey systems with elastic and inelastic behaviour. It was shown that the peak displacement demand at resisting planes equidistant from the geometric center may be similar if the damper is optimally placed. The torsional amplification of the edge displacements of arbitrary asymmetric structures relative to the displacements of their symmetric counterparts varied by about a factor of 2. Frictional dampers were equally effective in controlling the lateral-torsional coupling of both torsionally flexible and stiff structures. Using the optimal criteria maintained a similar maximum displacement at both edges of the building plan, which is less than twice the response of the nominally symmetric counterpart; in many cases, this can be controlled by adding more frictional capacity (Llera *et al.*, 2005).

Rofooei and Ebrahimi (2007) studied six and eight storey, 3D base-isolated structural models with LRB isolators with a variety of effective periods and damping ratios. The International Building Code (ICC, 2003) analysis procedure for the base-isolated structures was used to determine the minimum lateral seismic force and its vertical distribution at different floors. Nonlinear dynamic analysis was performed for eight types of LRB isolators; both the superstructure and the isolators were allowed to behave nonlinearly in order to evaluate the seismically induced demand shear force on different floors. The results indicated that the International Building Code (ICC, 2003) provisions suitably predict the seismic lateral forces for base-isolated buildings. However, they do not provide a good estimate of the shear force distribution over the height, especially for highly damped base-isolation systems (Rofooei and Ebrahimi, 2007).

In the preceding review, the differences in results indicate that the conclusions of the aforementioned studies are not generally applicable, but are restricted to the particular systems considered and the underlying modeling assumptions. Hence, there is a need for a more comprehensive and systematic investigation. Most studies have been conducted on single-storey structures subjected to similar earthquake records. The only studies that considered multi-storey buildings on elastomeric bearings are those of Nagarajaiah *et al.* (1993) and Tena-Colunga and Gómez-Soberón (2002).

The excessive displacement and ductility demand that may be generated in some of the elements during the post-elastic behaviour of such buildings under large earthquakes were not adequately accounted for in the design provisions. Asymmetric failure of torsional resisting elements is important, as this increases the structural eccentricity by shifting the center of rigidity away from the center of mass, increasing the damage and movement of the vulnerable elements. An interaction between lateral and torsional motions could also occur in base-isolated structures subjected to lateral ground motions when an eccentricity exists either in the superstructure or in the isolation system itself. The aim of this study is to determine whether a base isolation system is capable of reducing the torsional amplification of mass eccentric superstructures subjected to translational earthquake excitations. Furthermore, it is shown that having the base isolation system's center of stiffness coincide with the superstructure's center of mass is very effective in reducing the relative edge displacement, storey rotation and damage. The influence of rubber bearings' dynamic properties on the seismically coupled torsional response of asymmetric superstructures is also investigated.

EVALUATION OF PLAN CONFIGURATION

When a structure is subjected to a strong motion, the structural energy can be conceptually expressed as:

$$KE+DE+SE = IE \quad (1)$$

where, KE indicates the kinetic energy, DE is the dissipated energy, SE is the strain energy and IE is the seismic input energy. DE is the sum of VE and HE, which are the viscous and hysteretic energies, respectively.

In Eq. 1, KE and SE are the portions of the structural energy that are recoverable, whereas VE and HE are the portions that are dissipative. When the input energy cannot be dissipated via the viscous damping of the structure, the residual energy will be dissipated in the form of HE for strong motions. Energy input to a fixed-

base structure will be dissipated in the form of VE if IE is not too large. In the ductile design of fixed-base structures, plastic deformations may occur in several joints or members when the structure is subjected to strong motion and there is sufficient ductility such that collapse is prevented. The lateral motion of the system is coupled with the torsional motion under horizontal ground excitation when the center of stiffness of the elastomeric bearings does not coincide with the center of mass of the deck. Simplified base-isolated model is introduced to estimate torsional behaviour of seismic isolation with different superstructure plan configuration. Thus, four plans are selected and compared, it is observed that there is considerably more variation in the torsional to lateral frequency ratio in the L-plan (case 4) in comparison with the other cases (Fig. 1). Therefore, this type of plan is suitable for the study of the torsional

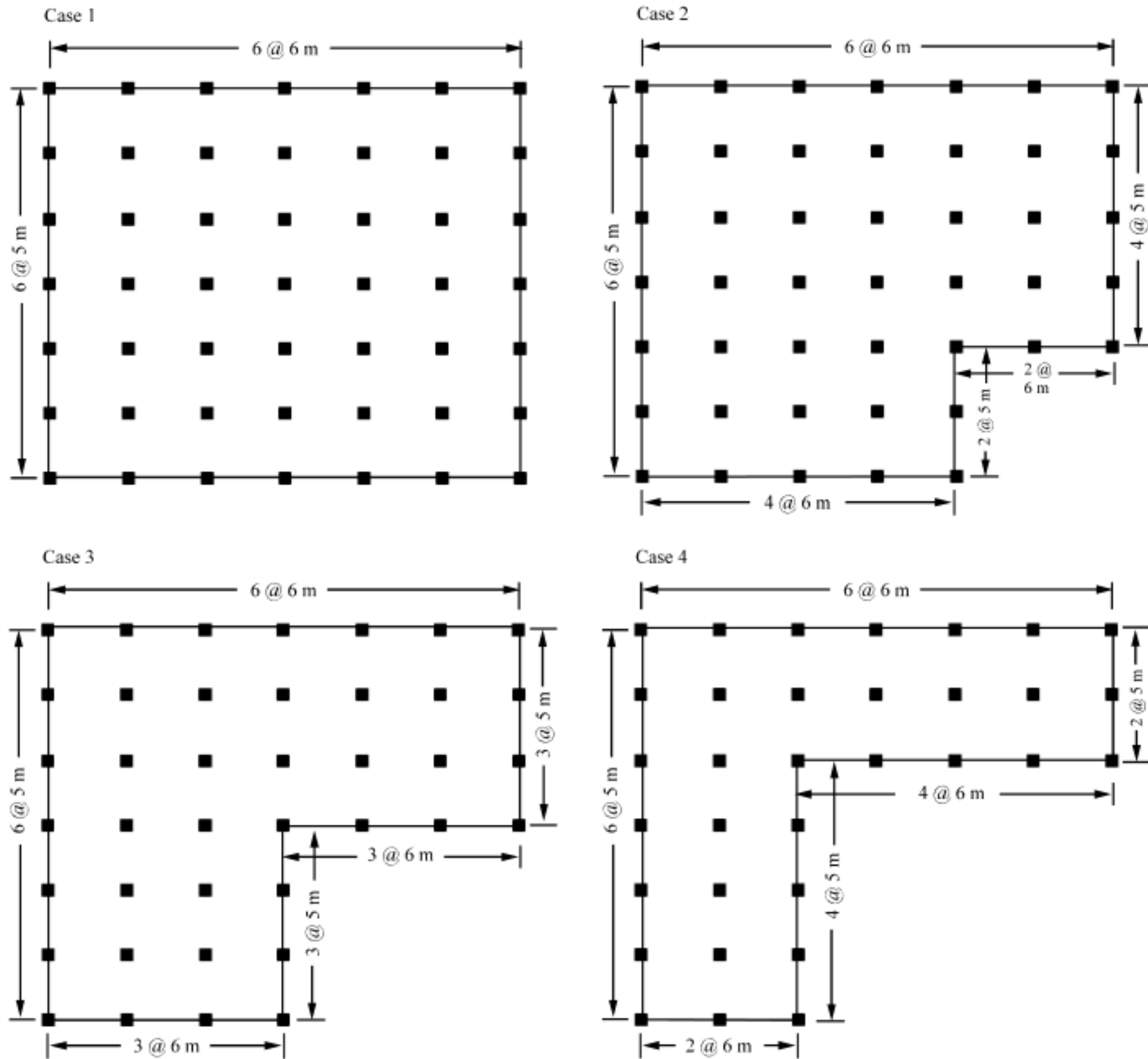


Fig. 1: Configurations of the four plans

behaviour of isolated structures. There is more eccentricity in case 4 relative to the other cases, so shifting the Center of Mass (CM) toward the CS generates a higher torsional response and the structural torque is reduced to a minimum if the center of stiffness of the isolation system coincides with the center of mass of the structure. Case 1 is a system with a symmetric distribution of mass and identical isolators distributed regularly in the building plan. The torsional to lateral frequency ratio varies when the CM is shifted toward the CS in cases 2, 3 and 4 for the same distributed total mass. As a result, the torsional resistance in asymmetric base-isolated structures will be increased when the elastomeric bearings in the exterior of the plan are stiffer and larger than interior or rubber bearings which are used in the interior and lead rubber bearings in the exterior. The torsional to lateral frequency ratio is computed in four cases of eccentricity in the base and for a rigid diaphragm level. The total distributed mass is constant but relative to the plan geometry characteristics and the rotational mass moment of inertia varies. The results of the computed frequency ratios indicate that case 4 is affected more by the torsional components; therefore the plan configuration of case 4 is a suitable selection for this purpose.

The structure on the base isolation system is idealized as a rigid deck with masses lumped at the corresponding column positions as shown in Fig. 2a. A parametric study is performed on the L-plan (case 4) with eccentricity in both horizontal directions at the base and the rigid diaphragm level. Case 1 to 3 can be simulated by changing the eccentricity and rotational mass moment of inertia; because the lateral mass and stiffness are assumed to be constant, the lateral frequency is restricted to 2.53 Hz. The mathematical characteristics of the base isolation system and superstructure are described as two

rigid diaphragms with three DOF in each level, including two translational and one torsional, attached to the CM of the rigid diaphragm (Fig. 2b). The isolator provides the base motions relative to the ground in two lateral directions. As shown in Fig. 2b, the translational displacement of the CM relative to the ground is defined by u_x and u_y . Rigid slab rotation around the vertical axis through the center of mass is defined by θ .

The translational stiffness of each isolation system in the x and y directions are K_x^i and K_y^i , respectively. It should be noted that $K_x^i = K_y^i = K_i$, when elastomeric rubber bearings are used in an isolation system. The total translational stiffness of the bearings in the x and y directions are:

$$K_{ix} = \sum_{i=1}^N K_x^i \tag{2}$$

$$K_{iy} = \sum_{i=1}^N K_y^i \tag{3}$$

$$K_{i\theta} = \sum_{i=1}^N K_x^i \cdot y_i^2 + \sum_{i=1}^N K_y^i \cdot x_i^2 \tag{4}$$

Thus, X_i and Y_i denote the distance of the i th bearing measured from the center of mass along the x and y axis, respectively. The center of stiffness of the elastomeric bearings is denoted by a point through which force can pass in any horizontal direction. The location of the center of stiffness relative to the center of mass at the base level is denoted by e'_x and e'_y :

$$e'_x = \frac{1}{K_y} \sum_{i=1}^N K_y^i \cdot x_i \tag{5}$$

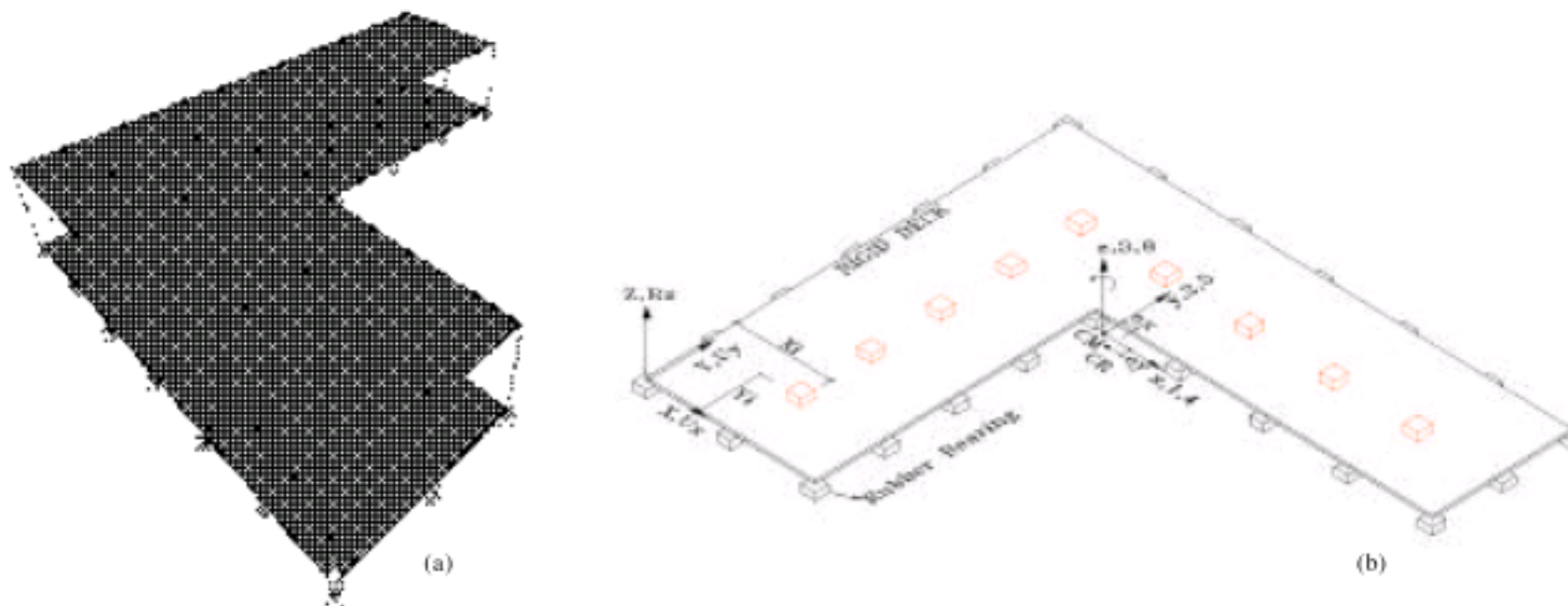


Fig. 2: (a) Simplified superstructure with base isolation system and (b) location of bearings in the isolation system

$$e'_y = \frac{1}{K_{ix}} \sum_{i=1}^N K_{ix}^i \cdot y_i \quad (6)$$

The total mass carried out by the isolation system (M) and the rigid diaphragm's moment of inertia is:

$$M = \sum_{i=1}^N m_i \quad (7)$$

$$I_\theta = \sum_{i=1}^N m_i \cdot (x_i^2 + y_i^2) \quad (8)$$

Let K_{sx} , K_{sy} and e_x , e_y be the superstructure's translational stiffness and eccentricity in both horizontal directions. Then, the equation of motion under earthquake loads is:

$$[M] \{\ddot{u}(t)\} + [C] \{\dot{u}(t)\} + [K] \{u(t)\} = -[M]\{r\} \ddot{x}_g(t) \quad (9)$$

where, M is mass, C is damping, K is the stiffness matrix with N×N dimensions and r is the influence coefficient vector.

The damping is assumed to be proportional to the mass and stiffness. The equation for the frequency of the system is denoted by Eq. 10 and its solution leads to Eq. 11, which is an algebraic polynomial equation with a degree of N.

$$\| -\omega^2 [M] + [K] \| = 0 \quad (10)$$

$$(\omega^2)^N + a_1 (\omega^2)^{N-1} + a_2 (\omega^2)^{N-2} + \dots + a_N = 0 \quad (11)$$

$$\Rightarrow \omega_1 < \omega_2 < \dots < \omega_N < \dots < \omega_N$$

The mass and stiffness matrices are developed in Eq. 12.

$$M = \begin{bmatrix} m_1 & 0 & 0 & 0 & 0 & 0 \\ 0 & m_1 & 0 & 0 & 0 & 0 \\ 0 & 0 & m_\theta & 0 & 0 & 0 \\ 0 & 0 & 0 & m & 0 & 0 \\ 0 & 0 & 0 & 0 & m & 0 \\ 0 & 0 & 0 & 0 & 0 & m_\theta \end{bmatrix}, \quad (12)$$

$$K = \begin{bmatrix} K_{ix} + K_{sx} & 0 & -K_{ix}e'_y - K_{sx}e_y & -K_{sx} & 0 & K_{sx}e_y \\ 0 & K_{iy} + K_{sy} & K_{iy}e'_x + K_{sy}e_x & 0 & -K_{sy} & -K_{sy}e_x \\ -K_{ix}e'_y - K_{sx}e_y & K_{iy}e'_x + K_{sy}e_x & K_{i\theta} + K_{s\theta} & K_{sx}e_y & -K_{sy}e_x & -K_{s\theta} \\ -K_{sx} & 0 & K_{sx}e_y & K_{sx} & 0 & -K_{sx}e_y \\ 0 & -K_{sy} & -K_{sy}e_x & 0 & K_{sy} & K_{sy}e_x \\ K_{sx}e_y & -K_{sy}e_x & -K_{s\theta} & -K_{sx}e_y & K_{sy}e_x & K_{s\theta} \end{bmatrix}$$

where, m and m_θ are the translational and torsional total mass of the superstructure, respectively.

Table 1: Torsional to lateral frequency ratios for cases 1 to 4 (Hz)

Case	Torsional frequency	Ratio of torsional to lateral frequency
1	2.29	0.91
2	2.26	0.89
3	2.12	0.84
4	1.86	0.74

The torsional stiffness of each isolator and its mass are negligible and are not included. Results of the frequency analysis and the torsional to lateral frequency ratios are shown in Table 1. The input data for evaluating the parametric study. In a system with many isolators, the frequency ratio is limited to 1 and the eccentricity is close to zero (Ryan and Chopra, 2004).

A comparison of the results indicates that the L-plan (case 4) is affected most by torsion and is therefore selected in the next section to evaluate the torsional response of base-isolated structures.

VERIFICATION

In order to verify the accuracy of the analytical results, an experimental five storey model (Samali *et al.*, 2003) is simulated using the SAP 2000 finite element software and the results are compared to the experimental studies. The measured stiffness and damping properties of the isolators are used for modeling the LRB system. In the finite element model, all of the joints are assumed to be fixed, but in reality these joints are not fully fixed; this difference can generate errors. Both fixed base and isolated structures with the LRB system are modeled with the software. In order to reduce the amount of output data, the two ground motions used by Hachinohe and Kobe are selected. The experimental building model has dimensions of 15×10×30 m and was designed by Samali *et al.* (1999). The original structural model, called the bare frame model, consists of five identical rectangular storeys of equal floor height, as shown in Fig. 3a (Samali *et al.*, 2003).

The superstructure is made of two moment-resisting frames in the longitudinal direction and three frames in the transverse direction and is subjected to seismic ground motion along the longitudinal direction. Figure 3b shows a mass eccentric model, which is generated by adding a total mass of 350 kg to one side of the bare frame. This excessive mass is created by 140 circular steel disks, which are distributed equally on the front side of each floor. Therefore, an eccentricity of 0.125 L is generated, where, L is the width of the floor. This level of eccentricity is classified as moderate eccentricity (Samali *et al.*, 2003). The isolated system consists of rubber bearings on each corner of the model (Fig. 3b). The dimensions of the laminated rubber bearings are 120×120×100 m. The shake

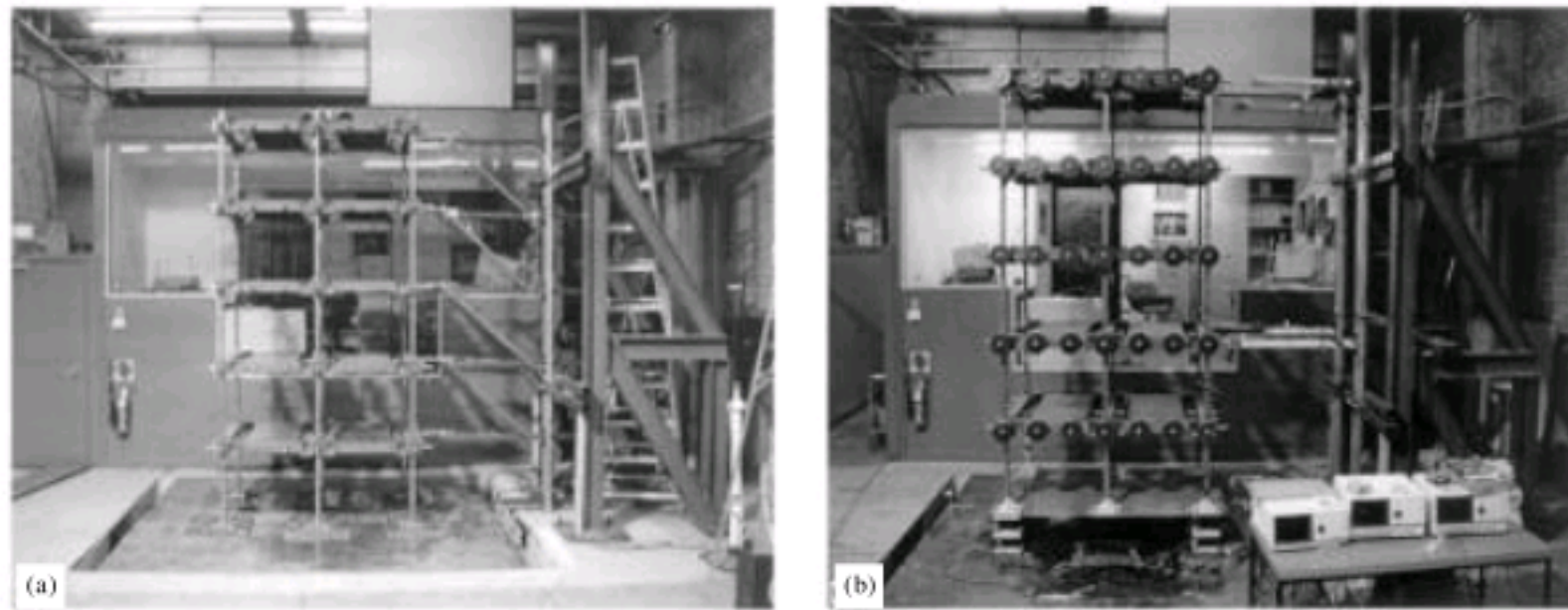


Fig. 3: (a) Concentric bare frame and (b) eccentric base-isolated frame (Samali *et al.*, 2003)

Table 2: Comparison of the lateral and torsional frequencies of the experimental and analytical models

Frequencies (Hz)	Mode					
	1st	2nd	3rd	4th	5th	6th
Bare frame (translational) (Exp.)	6.82	20.28	32.49	43.18	50.09	-
Bare frame (torsional) (Exp.)	8.63	25.68	41.57	55.00	63.87	-
LRB system (translational) (Exp)	2.51	12.15	22.20	33.98	42.55	49.90
LRB system (torsional) (Exp.)	3.36	14.92	25.82	40.98	53.64	63.31
Bare frame (translational) (FE)	7.02	20.88	33.97	45.09	52.76	-
Bare frame (torsional) (FE)	8.21	24.40	39.71	52.71	61.67	-
LRB system (translational) (FE)	2.48	13.52	24.50	38.00	47.30	55.80
LRB system (torsional) (FE)	3.05	15.88	28.20	45.07	55.06	63.80
Error (%)						
Bare frame (translational)	3	3	5	4	5	-
Bare frame (torsional)	5	5	5	4	4	-
LRB system (translational)	1	11	10	12	11	12
LRB system (torsional)	10	6	9	10	3	1

table is driven in the longitudinal direction of the five storey model. The maximum accelerations measured by Hachinohe and Kobe for earthquakes on a shake table were 0.23 and 0.41 g, respectively. The computational results for the natural frequencies of the experimental and Finite Element (FE) models for the bare frame and LRB systems with torsional and lateral effects are shown in Table 2. There is general agreement between the two sets of results, especially for the bare frame. The maximum error of this comparison is less than 12% for the LRB system (translational) in the 4th and 6th modes. The difference in the frequency results can be related to the configuration of LRB bearings, the details of their connections to the shaking table, the behaviour of the rubber in the actual model in comparison with the FE model and its stiffness distribution. Joint connections in the analytical model are assumed to be fixed, but there is no fully fixed connection in the actual model, which causes deviations from the experimental model results.

The maximum relative displacement of each storey for the bare and isolated models subjected to the Hachinohe and Kobe earthquakes are shown in Fig. 4a and b. The

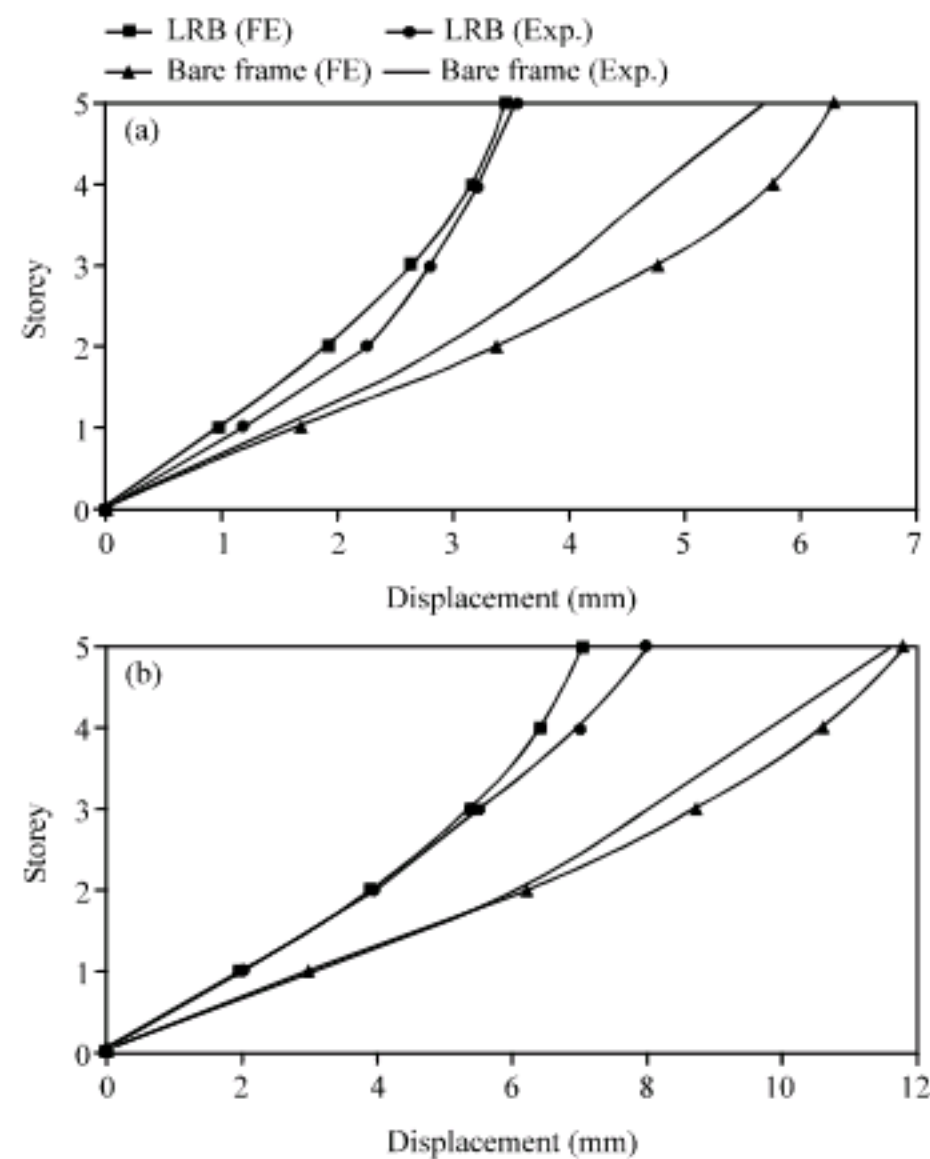


Fig. 4: Comparison of maximum relative displacements, (a) Hachinohe time history and (b) Kobe time history

results show a general agreement between the maximum of the experimental and analytical relative displacements.

Both of the experimental and analytical models have similar behaviours, especially in the lower storeys. Figure 5a and b compare the relative rotations in both the experimental and analytical cases. Relative rotation is used to characterise the torsional behaviour of the model and is defined as the relative rotation of the rigid diaphragms of the model. Again, the results are in good agreement.

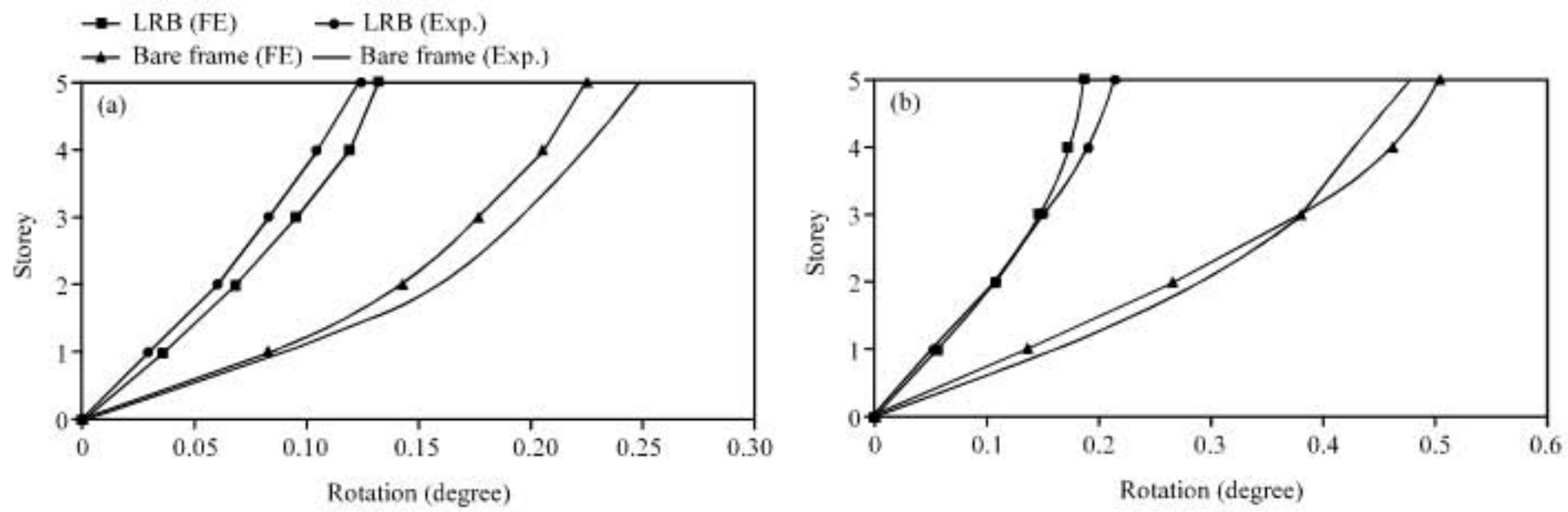


Fig. 5: Comparison of relative rotations, (a) Hachinohe time history and (b) Kobe time history

STRUCTURAL MODELS AND ISOLATION SYSTEMS

Figure 6a and b show a five storey 3D steel structure with asymmetry in both horizontal directions. The storey masses are assumed to be lumped at the floor levels. The magnitude of the lumped masses is proportional to the load carried by the corresponding columns. The superstructure consists of seven moment resisting frames in two directions, where the bay distance in one direction is 6.0 m and in the other direction is 5.0 m and the height of each storey is 3.0 m. The number of storeys and the plan dimensions were selected to approximate typical buildings. Three degrees of freedom in each floor (two translational and one torsional) are attached to the CM of the rigid diaphragm. The total mass corresponding to the CM of each storey is 40 t. The superstructure eccentricities in the L-shape plan of the building are set at 5 to 30% of the plan dimensions in the superstructure, as shown in Fig. 6.

The superstructure was originally designed as a fixed-base structure according to the seismic design specifications of the International Building Code (ICC, 2003) and the reduction of force demand due to the incorporation of the base isolation system was not considered. The CS of the bearing system generally does not coincide with the CM of the rigid diaphragm. The lateral motion of the system is coupled with the torsional motion under horizontal ground excitation. The stiffness distribution of the columns and bearings are asymmetric in both directions. Furthermore, the isolator is assumed to carry the vertical load without undergoing any vertical deformation. The superstructure eccentricities for this study are varied by shifting the CM away from the CS towards the left. A schematic plan view of the superstructure is also shown in Fig. 6. Elastomeric bearings represent a common means of introducing flexibility into an isolated structure. They consist of thin

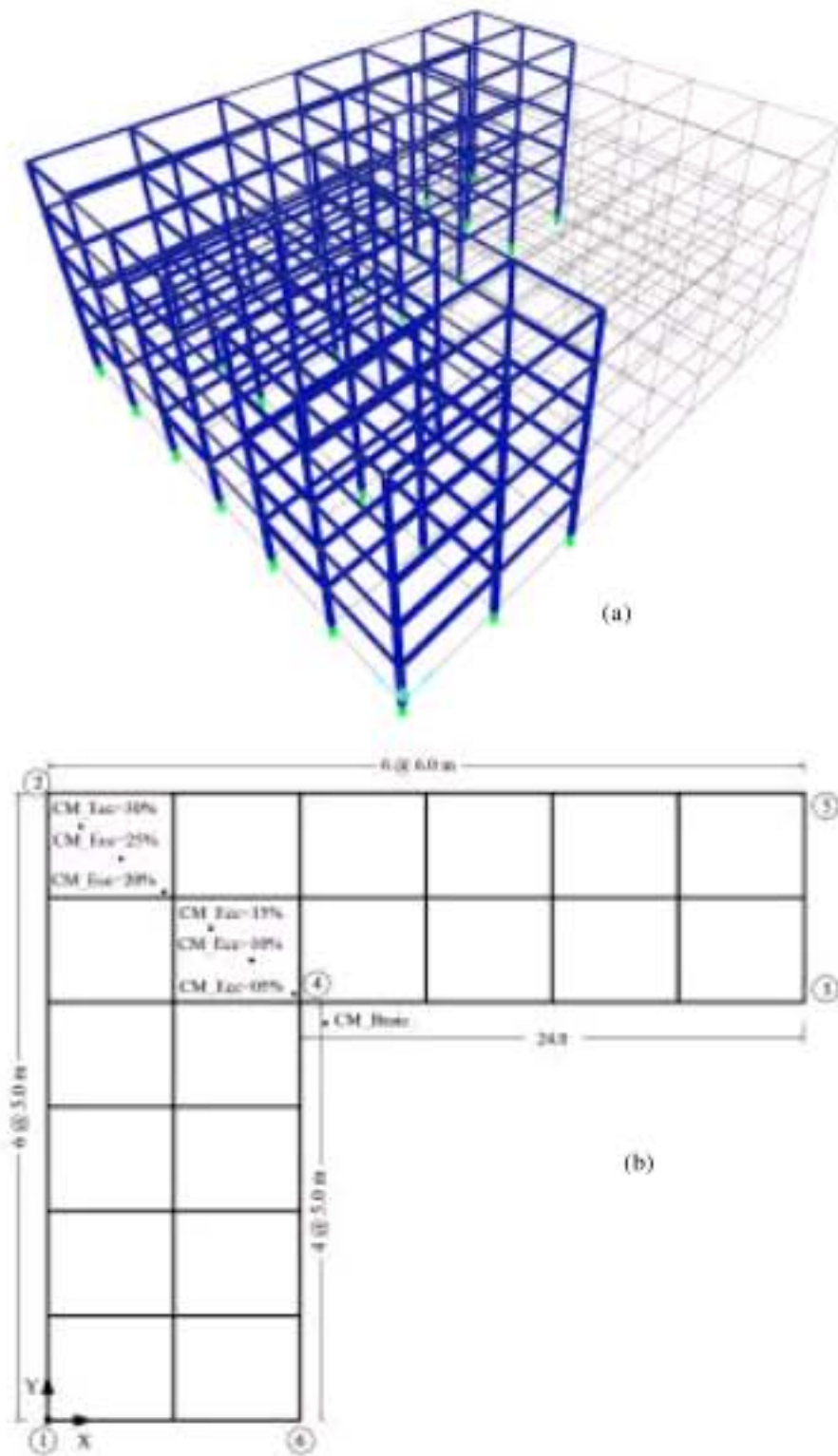


Fig. 6: 3D structure view and its typical plan (a) 3D view and (b) typical plan

layers of natural rubber that are vulcanised and bonded to steel plates. Natural rubber exhibits a complex mechanical behaviour, which can be described simply as a

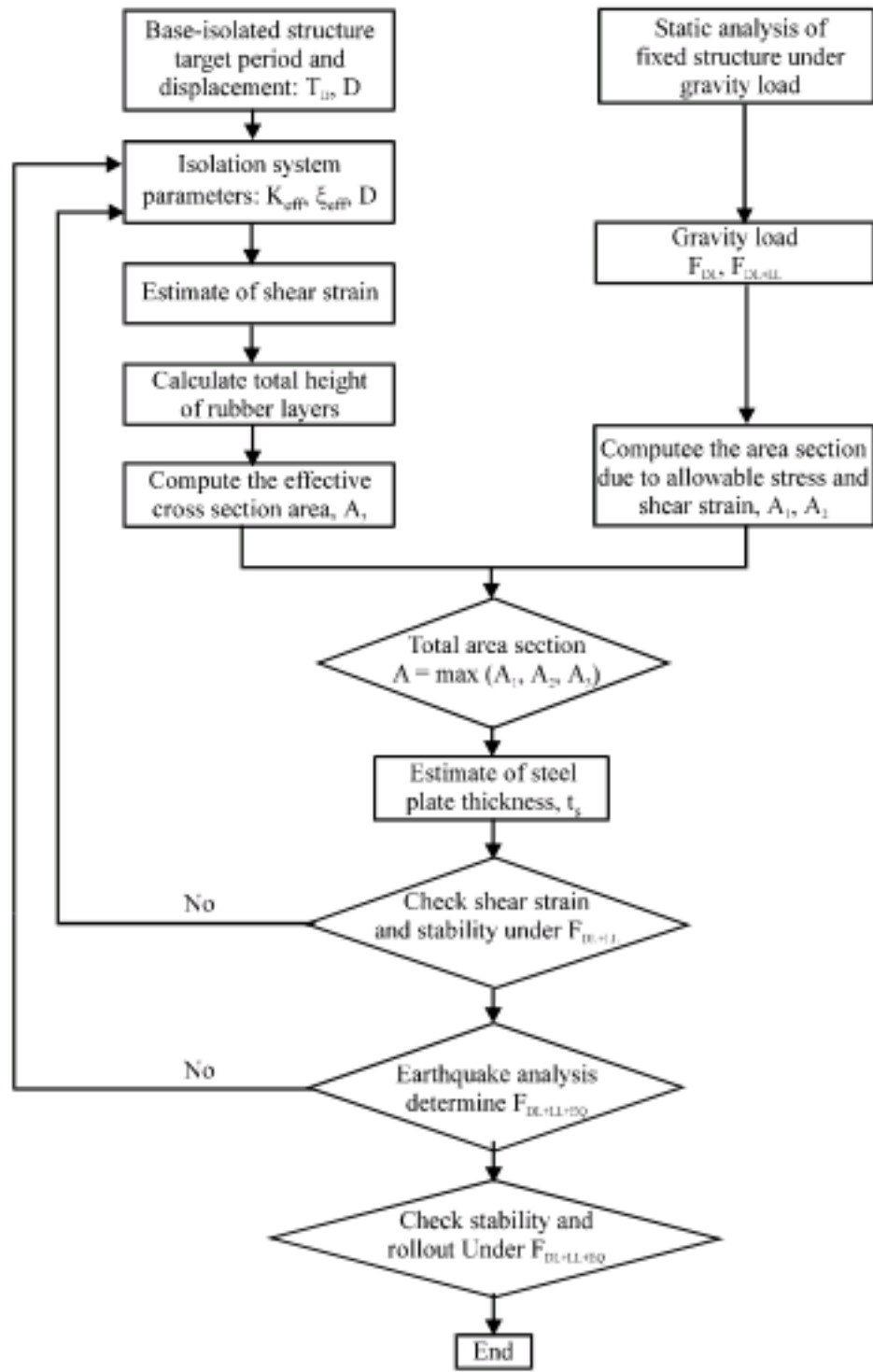


Fig. 7: Design flow chart for elastomeric rubber bearings

Table 3: Bearing characteristics

Bearing type	K _{eff} (kN m ⁻¹)	K ₁ (kN m ⁻¹)	F _y (kN)	Diameter (cm)	Height (cm)
A	285	2300	23	30	20
B	525	4200	42	40	20
C	769	6200	62	48	20
D	1021	8200	82	55	20

combination of viscoelastic and hysteretic behaviour. The isolation system was composed of 33 circular elastomeric bearings between the base of the superstructure and its foundation; the properties of the bearings are shown in Table 3. The LRBs were reinforced with steel plates, which support the vertical load and provide the lateral flexibility and energy dissipation capacity for the elastomeric isolation system used in this study. The design of the bilinear elastomeric isolation system is based on the provisions of the IBC 2003. The design flow chart for the elastomeric rubber bearings is shown in Fig. 7 and consists of steps such as: (1) determine the soil condition for the base-isolated structure, (2) select the effective damping ratio and shear strain for the bearing and the target design period of the base-isolated structure, (3)

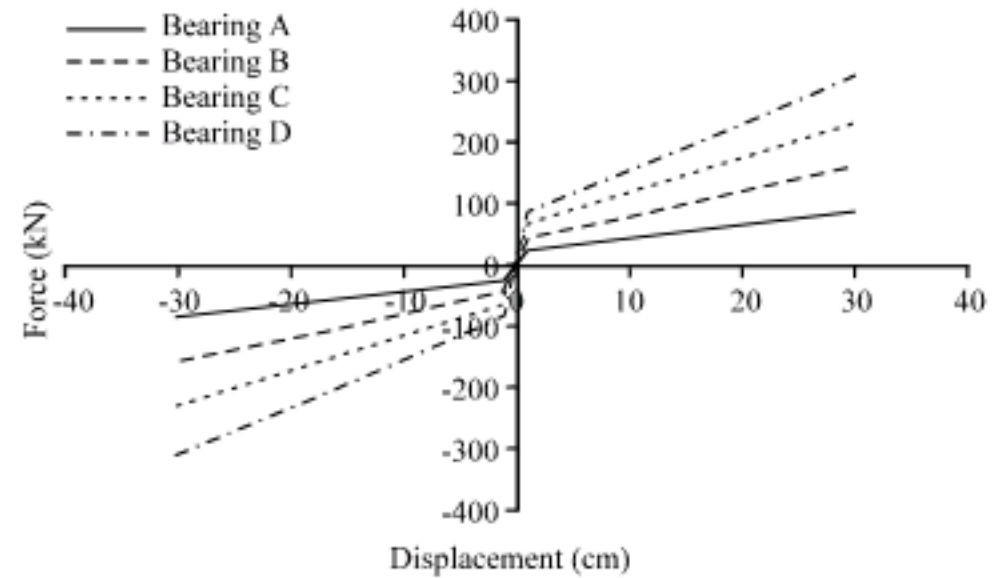


Fig. 8: Force displacement properties of isolation systems

use static and dynamic analysis to determine the maximum design displacement and effective horizontal stiffness of the bearings, (4) select the material characteristics, such as shear and Young modulus, from the experimental test report and (5) calculate the height of the rubber in the bearing according to the design shear and displacement.

Figure 8 shows the force-displacement characteristics of the isolation systems modeled assuming bi-linear behaviour with three attributes, namely: (1) post-to pre-yielding stiffness ratio, (2) yield displacement and (3) effective stiffness. The post-yield stiffness of the isolation system is generally designed to provide the specific value of the isolation period, expressed as:

$$T_b = 2\pi\sqrt{M/K_b} \tag{13}$$

$$M = \left(m_b + \sum_{j=1}^N m_j \right) \tag{14}$$

where, M is the total mass of the base isolated structure and m_j is the mass of the jth floor of the superstructure.

Relative to torsional effects, the design displacements are varied in different eccentricities and Fig. 8 shows the force displacement properties for the original case with minimum eccentricity.

The total design displacement of the elastomeric bearings with respect to the torsional displacement and the corresponding eccentricities, are computed for each structure. The results show that the force displacement characteristics of the isolation systems are variable as the eccentricity increases.

The inter-storey drifts were limited to 0.015/R₁, where the R₁ factor for the steel moment resistant frame is 2.0, as prescribed by the IBC 2003.

GROUND MOTIONS

Several typical earthquakes of variable frequency are used in this study and the average responses for the

Table 4: Characteristics of ground motion excitations

Earthquake	Stations	Year	Component	PGA (g)	PGV (cm sec ⁻¹)	PGD (cm)
Loma Prieta	Hollister	1989	0	0.369	62.78	30.18
			90	0.178	30.89	20.42
Loma Prieta	Lexington Dam	1989	0	0.442	84.43	14.67
			90	0.409	34.98	25.81
Imperial Valley	Array No. 6	1979	230	0.436	100.71	55.17
			140	0.376	63.13	26.94
Landers	Lucerne Valley	1992	L	0.703	25.72	8.82
			T	0.665	68.44	28.22
Petrolia	Petrolia	1992	0	0.589	48.30	15.24
			90	0.662	89.45	30.58
Northridge	Sylmar	1994	90	0.604	76.49	15.22
			360	0.843	128.88	32.55
Landers	Yermo Fire	1992	270	0.245	50.81	41.28
			360	0.151	29.03	22.78

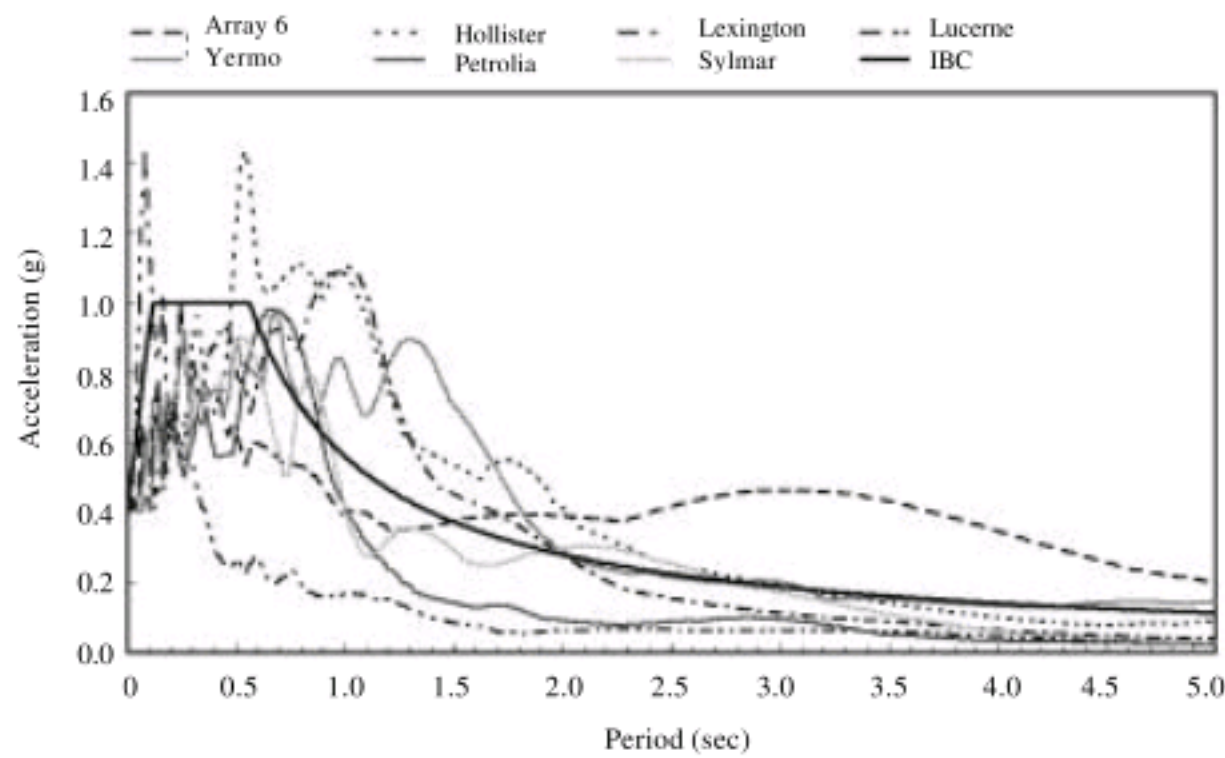


Fig. 9: Acceleration response spectra of ground motion components

selected records are determined according to the IBC 2003 code. Seven ground motion records were selected from the California Division of Mines and Geology database (CDMG). The data in Table 4 include the earthquake name, peak ground acceleration and the velocities and displacements for the two horizontal components of each motion. The two horizontal components of the records are considered in this study. Based on the IBC code, in the case of using at least seven earthquake records, the average values obtained from the analyses for different response parameters can be used for design purposes.

Figure 9 shows the acceleration response spectra of the seven ground motion components in comparison with the International Building Code (ICC, 2003) design spectrum. Each component of motion is scaled to a PGA of 0.4 g. For each pair of horizontal ground motions, the square root of the sum of the squares (SRSS) of the 5% damped spectrum of the scaled horizontal components is constructed. Figure 10 indicates a close match between

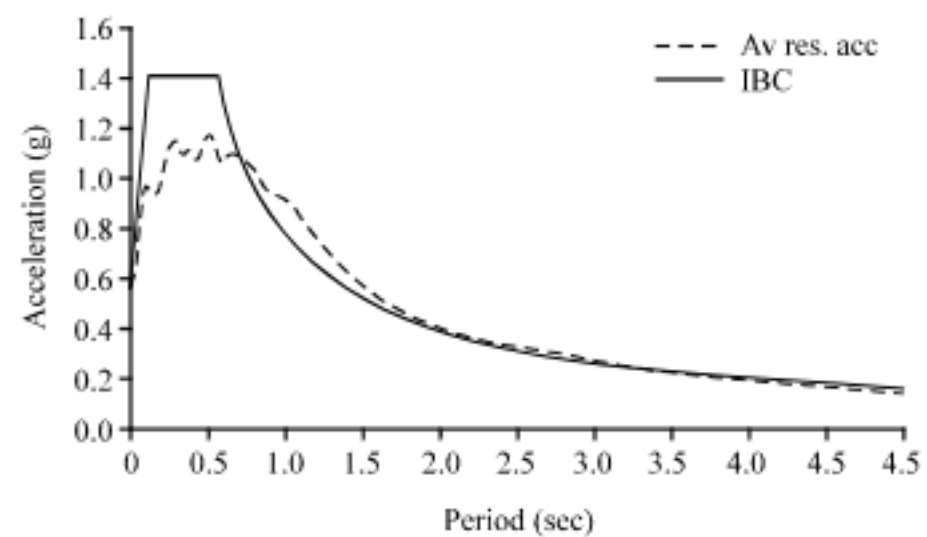


Fig. 10: Average value of the SRSS spectra and 1.4 times the spectrum of the design earthquake

the average SRSS spectrum of the scaled records and the IBC 2003 design spectrum, especially at longer periods, which are of key interest for base-isolated structures. Thus, it is observed that the average of the spectra is approximately 1.4 times the IBC 2003 design spectrum.

NONLINEAR DYNAMIC ANALYSIS

Nonlinear dynamic analyses are performed on the isolated structures using a bilinear model for both the isolation system and the superstructure members. The seven ground motion pairs shown on Table 4 are used for time history analysis. The duration of the time histories must be consistent with the magnitude and source characteristics of the earthquake design basis. The average values obtained from the analysis for different response parameters can be used to compare the results. The average SRSS spectrum of the scaled records and 1.4 times the 5% damped IBC 2003 design spectrum (Fig. 10) indicate a close match, especially at longer periods, which is the main range of interest for base-isolated structures. International Building Code (ICC, 2003) requires that the average SRSS spectrum not fall below 1.3 times the design spectrum by more than 10%. The nonlinear time history analysis of the five storey fixed-base structure were performed considering nonlinear behaviour for different structural elements of the model and the simultaneous application of both components of each pair of earthquake records to the structural model.

RESULTS OF ANALYSIS

This study investigates the dynamic analysis of an elastomeric isolation system consisting of laminated rubber bearings. The models are studied at degrees of structural eccentricity of 5, 10, 15, 20, 25 and 30% of the plan dimensions, for both directions, as shown in Fig. 6. Table 5 shows comparisons of the first three mode periods with a fixed base and isolated cases with that of a special base-symmetric case. Here, the base-symmetric case does not indicate a completely symmetric building and is constructed by having the CS of the bearings coincide with the CM of the superstructure at the base level. For this purpose, the stiffness of the bearings in the 1-2 and 2-5 edges of the L-plan (Fig. 6) is increased while the total lateral stiffness of the elastomeric bearings is kept constant. In practice, simply altering the dimensions of the rubber or its shear modulus can modify the stiffness of these bearings. This type of bearing distribution can be used to reduce the torsional responses. According to Table 5, the isolated structure in the first mode with symmetry in the base level is reduced, especially at higher levels of eccentricity. A study of the participating mass ratio demonstrates that the first mode cases with 10% and greater eccentricities have torsional behaviour, but the base-symmetry is reduced (Table 5). Furthermore, a similar period in the second and third modes indicates the effectiveness of the proper stiffness

Table 5: Comparison of the periods of the fixed base and isolation systems with the base-symmetric case (sec)

Ecc (%)	Mode	Fixed base	Isolation system	Case with symmetry at base level
Original case	1	1.12	2.47	2.48
	2	1.00	2.40	2.44
	3	0.96	2.38	2.37
5	1	1.14	2.61	2.51
	2	1.04	2.44	2.46
	3	0.92	2.36	2.23
10	1	1.22	2.88	2.62
	2	1.06	2.43	2.47
	3	0.87	2.09	2.44
15	1	1.34	3.21	2.93
	2	1.07	2.43	2.45
	3	0.83	1.99	2.44
20	1	1.48	3.61	3.07
	2	1.06	2.42	2.50
	3	0.80	1.91	2.45
25	1	1.61	4.04	3.65
	2	1.04	2.41	2.55
	3	0.78	1.86	2.46
30	1	1.76	4.47	4.06
	2	1.03	2.39	2.55
	3	0.76	1.82	2.48

distribution of the bearings when the CS of the bearings coincides with the CM of the superstructure in the base level.

Relative displacement and rotation are important parameters in evaluating dynamic responses, as well as in estimating the amount of damage. Comparisons of fixed and isolated structures with base-symmetric structures for three edges in both horizontal directions are shown in Fig. 11 and 12. In Fig. 11 and 12, the horizontal axis represents storey drifts and the vertical axis indicates the storey number. In this study, corner numbers 1 and 2 and 1 and 3 in the X and Y directions, respectively are selected to evaluate the relative displacements and seismic responses of asymmetric base isolated buildings. The base isolated drifts are significantly reduced in comparison with the corresponding fixed base models for all eccentricity levels, as shown in Fig. 11 and 12. The graph legends indicate the corner number and its direction for the three cases of (a) fixed base, (b) base isolated and (c) isolated structure with symmetry in the base level (the isolation system's CS coincides with the superstructure's CM). Torsional moments will be reduced when the CS of the bearings coincides with the CM of the superstructure in the base level. Displacement and damage reduction in the exterior edges is more obvious in this case than for the base isolated structure. It is concluded that the relative displacement reduction of edge 1 is greater than that for edge 2 in the X-direction and will occur in the base-symmetric case at higher levels of eccentricity (Fig. 11a-g). The situation is similar for edge 3 and 1 in the Y-direction (Fig. 12a-g). The top storey's relative displacement for the

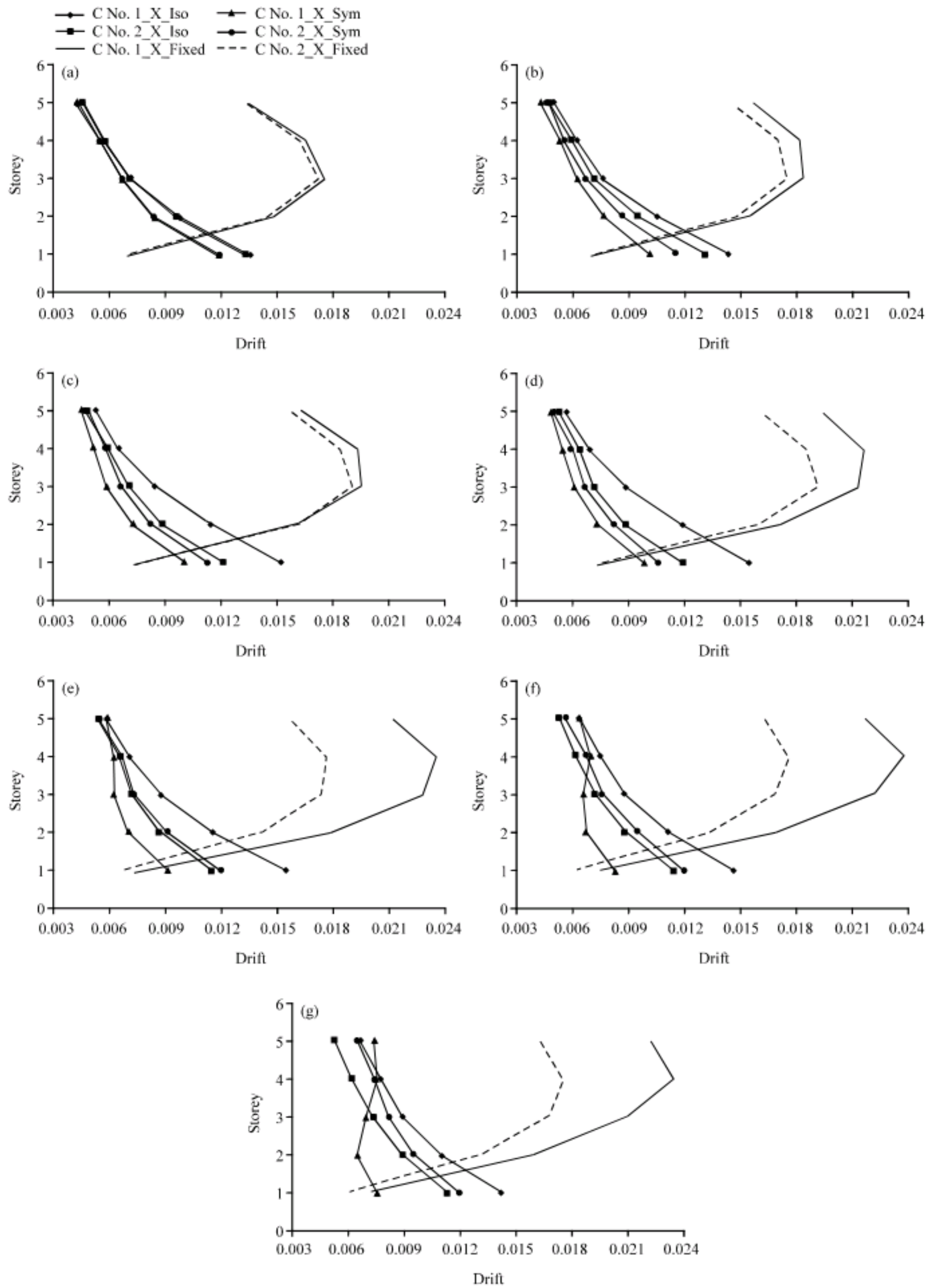


Fig. 11: Drift comparison of fixed and isolated structures with base-symmetric in 1 and 2 edges -X direction (a) original model, (b) 5%, (c) 10%, (d) 15%, (e) 20%, (f) 25% and (g) 30% eccentricity

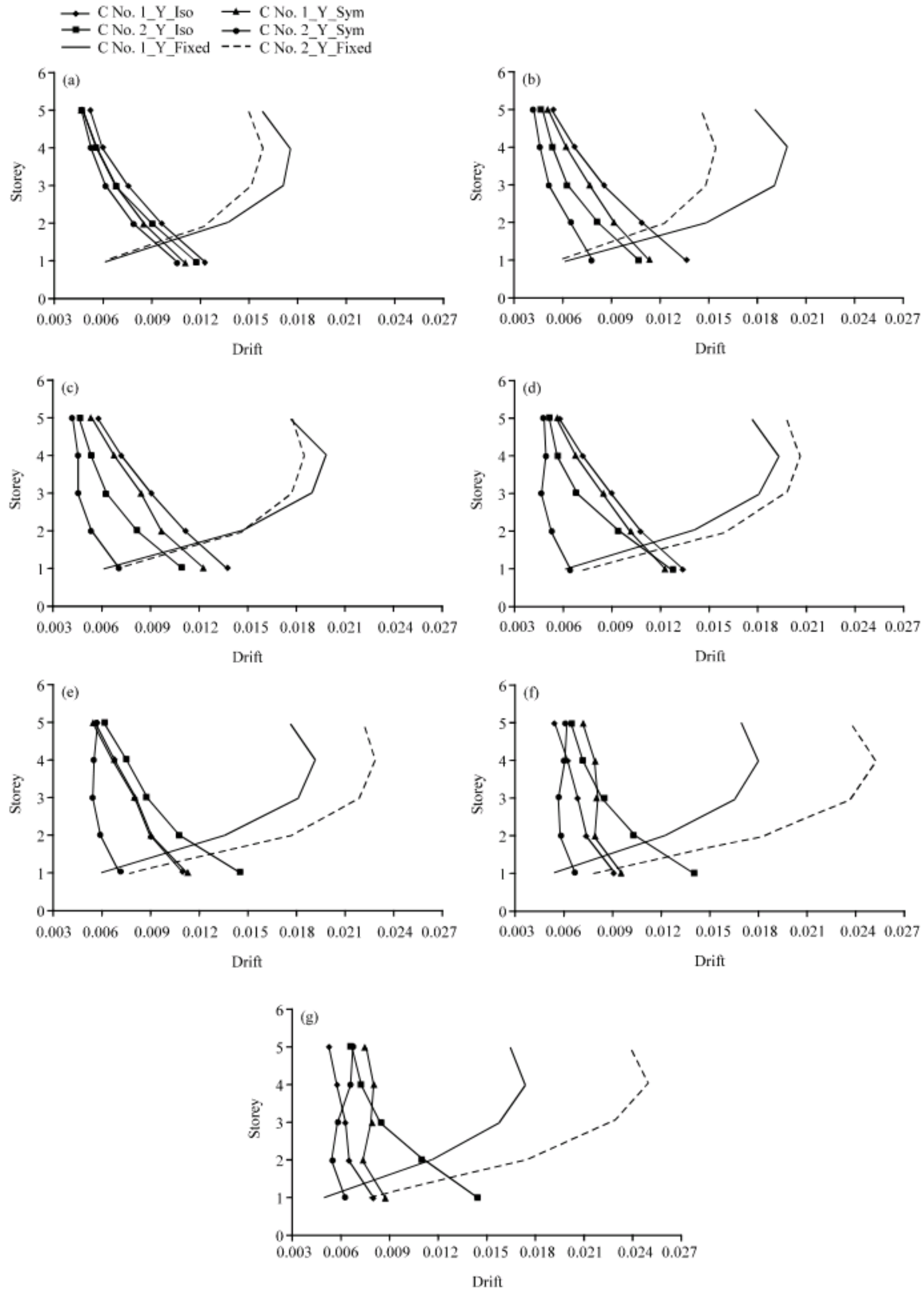


Fig. 12: Drift comparison of fixed and isolated structures with base-symmetric in 1 and 3 edges -Y direction, (a) original model, (b) 5%, (c) 10%, (d) 15%, (e) 20%, (f) 25% and (g) 30% eccentricity

base-symmetric condition is more uniform for edge 3 in the Y-direction compared with the corresponding edge 1 in the X-direction. Thus, the coincidence of the isolation system's CS with the superstructure's CM is highly effective in reducing the relative displacement for higher levels of eccentricity. It is observed in this case that both the translational and torsional responses are reduced and that eccentric structures are protected. In addition, uniform drifts are present in the upper storeys of the base-symmetric case. The symmetry of the isolation level in base isolated structures has little effect in reducing the storey drift at lower eccentricities. However, Fig. 11a shows that drift reduction in the lower storeys is greater than in the upper storeys. At higher levels of eccentricity, the coincidence of the CS of the bearings with the CM of the superstructure is more effective in reducing the responses than in other cases, such as the fixed base and isolated structure without symmetry in the base (Fig. 11b-g). As shown in Fig. 11e-g, storey drift is uniformly distributed along the height in the base-symmetric case, even if the superstructure eccentricity is large; this is more obvious in corner 1, with 20, 25 and 30% eccentricity levels. In the base-symmetric case, storey drift is reduced in corners 1 and 2, since increasing the bearing stiffness in the exterior edges (1-2 and 2-5) causes the excessive torsional stiffness to eliminate the torsional moments and enhance the performance of the eccentric base-isolated structures. For the fixed and isolated base conditions, storey drift reduction is observed in corners 1 and 2 along the height of the structure at 5 to 15% eccentricity levels. The total lateral stiffness of the bearings for the base-symmetric case is constant and equal to case of the base isolated building without the coincidence of the CS of the bearings with the CM of the superstructure. There is similar behaviour in the storey drift of edge 2 in the base-symmetry and isolated case at high levels of eccentricity (25 and 30%). However, as shown in Fig. 11f, storey drift variations are small and uniform along the height when compared with the isolated case without symmetry at the base level. For higher eccentricity levels, the storey drift reduction is not observed in edge 1 but it is distributed uniformly in storeys, as shown in Fig. 12f, g. In all cases, symmetry in the seismic isolation level reduces the response and enhances the performance.

The relative floor rotations of the fixed base, isolated structure and base-symmetric structure are shown in Fig. 13a-g. In Fig. 13, the horizontal axis indicates the relative floor rotation and the vertical axis shows the number of storeys. It should be noted that the relative rotation of the base-symmetric case is highly reduced compared with the other cases. The comparisons show

that storey rotation is uniformly distributed along the height in base-symmetric and isolated structures. It is observed that a reduction in the torsional response can be obtained by the proper placement of the elastomeric bearings in the isolation system, even for large structure eccentricity levels. The use of stiffer bearings in the exterior edges (1-2 and 2-5) reduces the eccentricity (distance between the CS of the isolation system and the CM of the superstructure), so that increasing the torsional stiffness results from the location of the bearings and its design. This increases the radius of gyration and the shear modulus. Asymmetric base-isolated structures can be improved by these factors without the need to strengthen the structural elements against torsional effects. There is a larger relative rotation reduction for the base-symmetric case at larger eccentricities, particularly in the upper storeys, because the distribution of the torsional moments is minimized by creating symmetry in the isolation level. In this case, the superstructure eccentricity between the CM and rigidity exists and is constant; however, the symmetry at the elastomeric bearings level exhibits superior response reductions and also causes uniform relative rotation and displacement in the asymmetric building plan against torsional effects. The isolation system is most effective when its CS coincides with the superstructure's CM; furthermore, the use of a bilinear hysteretic base isolation system is effective at reducing the effects of torsional moments in structures. Storey rotation is one of the important factors for evaluating the behaviour of eccentric structures and its reduction enhances the performance (Fig. 13a-g). The relative rotation is severely reduced in the lower storeys because the eccentricity of the superstructure exists at a higher level of the base. The elastomeric bearings should be stiffer at the exterior edges to generate more torsional stiffness to eliminate the effects of higher eccentricity. Storey displacement is another important response parameter, especially in the base level of base-isolated buildings. Displacement is also an essential parameter of elastomeric bearing design; thus, the horizontal displacement capacity in both plan directions is limited to the bearing's material and geometric characteristics. The maximum storey displacement of the base-isolated and base-symmetric structures in both dimensions is shown in Fig. 14. Figure 14 shows that the displacement reduction at different eccentricities occurs for the base-symmetric structure in both plan directions, but not for the isolated structure, although displacement increases with eccentricity. However, the maximum displacement of storeys at large eccentricities is more uniform, especially in the upper storeys. In addition, the symmetry at the base level considerably reduces the amount of displacement in

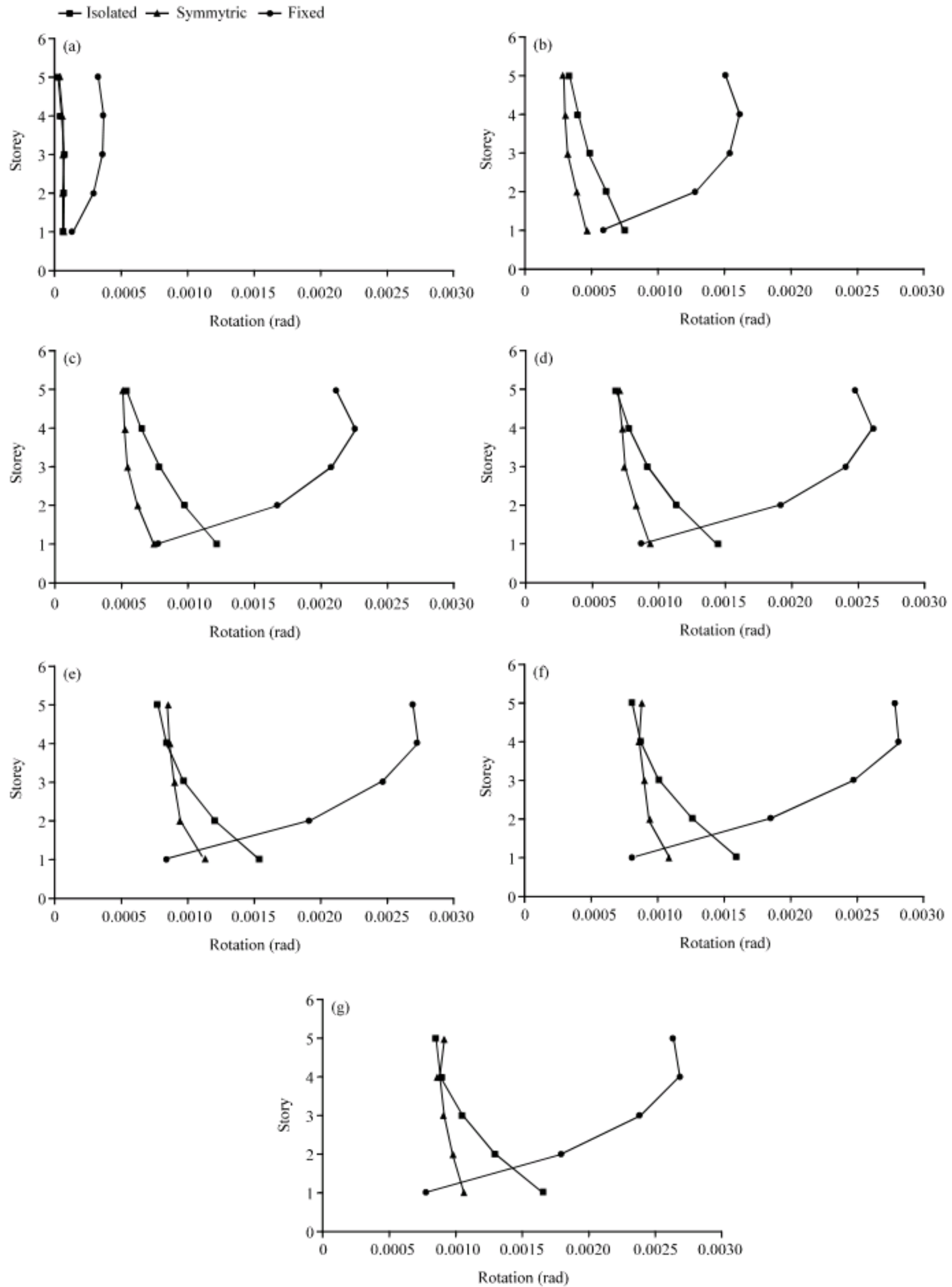


Fig. 13: Relative rotation of fixed, isolated and base-symmetric structures, (a) basic model, (b) 05%, (c) 10%, (d) 15%, (e) 20%, (f) 25% and (g) 30% eccentricity

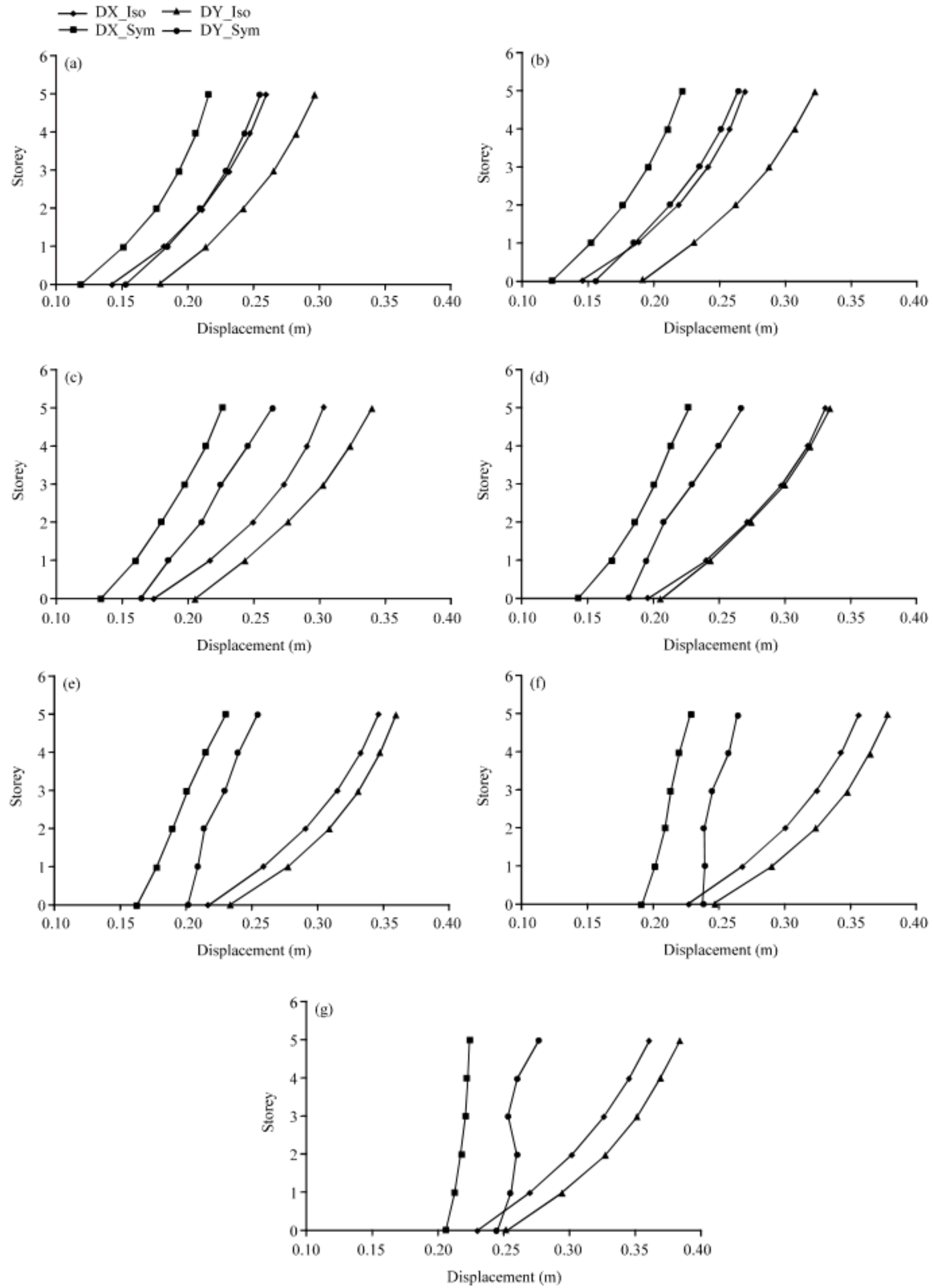


Fig. 14: Maximum displacement of the base-isolated and the base-symmetric structures, (a) basic model, (b) 05%, (c) 10%, (d) 15%, (e) 20%, (f) 25% and (g) 30% eccentricity

each storey (Fig. 14e-g). The reduction in structural and non-structural damage is directly related to the amount of storey displacement; therefore, symmetry in the base level will be a method for controlling damage in base-isolated buildings with eccentric superstructures. These results suggest that symmetry in the base level provides a reduction of torsional effects and responses in both the base-isolation system and superstructure. A symmetric base is constructed by focusing on the isolation level and is carried out by selecting the proper bearing locations; it is therefore not required to re-design elements of the superstructure to withstand torsional effects. Interaction between the lateral and torsional motions will not occur in base-isolated structures subjected to lateral ground motions, when an eccentricity does not exist at the base level. The main source of torsional motions in elastomeric isolated structures is the isolation system's eccentricity. Increasing the ratio of the dynamic torque to the static torque at the CS of a superstructure is related to increasing the isolation eccentricity (e_p/L).

CONCLUSIONS

The objectives of this study were to identify important base-isolation system characteristics, determine the proper location to reduce torsional effects and investigate the influence of various levels of eccentricity on the response parameters. The effectiveness of providing symmetry at different levels of the base isolation system was evaluated by comparing the translational and torsional responses of the model. This study confirms that symmetry in the base isolation level, which is developed when the isolation system's CS coincides with the superstructure's CM, can be very effective in reducing the responses of torsionally coupled systems, even for various superstructure eccentricity levels. The response reduction is greater in the lower storeys of the isolated structure, especially for the symmetric case at the base level. Additionally, it is observed that superstructure eccentricity has a significant influence on base isolation responses. Seismic isolation displacement increases with eccentricity level; therefore, having the bearings' CS coincide with the superstructure's CM can be used to generate a more uniform distribution of response along the building height. Structural torque was reduced with the base isolation system and this reduction is greater when the CS of the isolation system coincides with the CM of the superstructure. The asymmetric and dynamic characteristics of the superstructure are as important as those of the isolation system; thus, base isolation

displacements are affected by superstructure eccentricity. The main source of torsional motions in elastomeric isolated structures is the isolation system eccentricity. The isolator's eccentricity increases the base displacements and decreases the effectiveness of the isolation system to prevent torsional deformations. In addition, increasing the isolation eccentricity leads to increased torsional amplification. Symmetry (when the CS of the isolation system coincides with the CM of the superstructure) is more effective in the base level; it can also be used to retrofit vulnerable structures against torsional effects without replacing or reinforcing their elements. One advantage of this method is that the operations are concentrated only in the isolation level.

REFERENCES

- Almazan, J.L. and J.C. De La Llera, 2000. Lateral torsional coupling in structures isolated with the frictional pendulum system. Proceedings of the 12th world conference on Earthquake Engineering, New Zealand, Jan. 30-Feb. 4, New Zealand Society for Earthquake Engineering, pp: 1-1.
- Chandler, A.M., 1986. Building damage in Mexico City earthquake. *Nature*, 320: 497-501.
- Eisenberger, M. and A. Rutenberg, 1986. Seismic base isolation of asymmetric shear buildings. *J. Eng. Struct.*, 8: 2-8.
- ICC., 2003. International Building Code 2003. 2nd Edn., International Code Council Inc., USA., ISBN: 1-892395-79-7.
- Jangid, R.S. and T.K. Datta, 1994. Non-linear response of torsionally coupled base isolated structure. *J. Struct. Eng.*, 120: 1-22.
- Lee, D.M., 1980. Base isolation for torsion reduction in asymmetric structures under earthquake loading. *J. Earthquake Eng. Struct. Dyn.*, 8: 349-359.
- Llera, D., C. Juan, L. José Almazan and J. Ignacio Vial, 2005. Torsional balance of plan-asymmetric structures with frictional dampers: Analytical results. *J. Earthquake Eng. Struct. Dyn.*, 34: 1089-1108.
- Nagarajaiah, S., M. Andrei Reinhorn and C. Michalakis Constantinou, 1993. Torsion in base-isolated structures with elastomeric isolation systems. *J. Struct. Eng.*, 119: 2932-2951.
- Nakamura, T., T. Suzuki, H. Okada and T. Takeda, 1989. Study of base isolation for torsional response reduction in asymmetric structures under earthquake motion. Proceedings of the 9th world Conference on Earthquake Engineering, Aug. 3-9, 9WCEE Organization Commite, Japan, pp: 675-680.

- Pan, T.C. and J.M. Kelly, 1983. Seismic response of torsionally coupled base isolated structures. *J. Earthquake Eng. Struct. Dyn.*, 11: 749-770.
- Rofooei, F.R. and M. Ebrahimi, 2007. Evaluation of the vertical distribution of base shear force in base-isolated structures. *Sci. Iran.*, 14: 11-22.
- Ryan, K.L. and A.K. Chopra, 2004. Estimation of seismic demands on isolators in asymmetric buildings using non-linear analysis. *J. Earthquake Eng. Struct. Dyn.*, 33: 395-418.
- Samali, B., E. Mayol, J. Li and Y.M. Wu, 1999. System identification of a five storey benchmark model using modal analysis. *Proceedings of the International Conference on Applications of Modal Analysis*, Dec. 15-17, Gold Coast, Queensland, Australia, pp: 12-12.
- Samali, B., M. Wu Yi and J. Li, 2003. Shake table tests on a mass eccentric model with base isolation. *J. Earthquake Eng. Struct. Dyn.*, 32: 1353-1372.
- Tena-Colunga, A. and L. Gómez-Soberón, 2002. Torsional response of base-isolated structures due to asymmetries in the superstructure. *J. Eng. Struct.*, 24: 1587-1599.